NUCL SCI TECH (2021) 32:55
https://doi.org/10.1007/s41365-021-00899-7

Properties of Z =114 super-heavy nuclei

Yu-Qi Xin[1] · Na-Na Ma[1] · Jun-Gang Deng[1] · Tian-Liang Zhao[1] · Hong-Fei Zhang[1,2,3]

Received: 11 January 2021 / Revised: 12 April 2021 / Accepted: 29 April 2021 / Published online: 4 June 2021

Abstract The center of the stability island of super-heavy nuclei (SHN) is the subject of intense experimental and theoretical investigations and has potential technological applications. $^{298}_{114}$Fl lies in the Z =114 isotopic chain as a persuasive candidate of the spherical double-magic nucleus in SHN, and in this study, the calculations of nuclear binding energies, one-nucleon and two-nucleon separation energies, α-decay energies, and the corresponding half-lives provide strong evidence for this point. These calculations within an improved Weizsäcker-Skyrme nuclear mass model (WS*) were performed and compared with the calculations of the finite-range droplet model (FRDM2012) and experimental data for $Z = 114$ isotopes and $N = 184$ isotones. Concurrently, the corresponding single-particle levels in a Woods-Saxon potential well with a spin-orbit term are calculated, which can be used as a powerful indicator to identify the shell effects existing in $^{298}_{114}$Fl. Both the study of the properties of the isotopic chain and microphysical quantities provide a vital signal that $^{298}_{114}$Fl is a spherical double-magic nucleus and also the center of the SHN.

Keywords Super-heavy nuclei · Separation energy · Single-particle level · α decay

1 Introduction

According to nuclear theory, the limits of the existence of heavy nuclei, as well as their decay properties, are completely determined by nuclear shell effects. The α decay Q values and half-lives of the new nuclides with $Z = 104 - 118$ and $N = 162 - 177$ that have been synthesized in the complete-fusion reactions of ^{238}U, ^{242,244}Pu, ^{243}Am, and ^{245,248}Cm targets with ^{48}Ca beams indicate a considerable increase in the stability of super-heavy nuclei (SHN) with an increase in the number of neutrons [1–9]. The observed radioactive properties of these newly synthesized nuclei and the products of its α decay data, such as the trend in the α-decay energies of the already synthesized $Z = 114$ isotopes in Ref. [10, 11], can be considered as experimental proof of the "island of stability" approach of super-heavy elements around Z=114.

Theoretically, nuclear mass calculation with increasing precision has been pursued over the past decades [12–15], and consequently, great improvements have been made. The extrapolations based on the nuclear shell model performed in the 1960s led to the prediction of a magic stability island surrounding the double-magic nuclear number $Z = 114$ and $N = 184$ [16–18]. In purely microscopic

This work was supported by the National Natural Science Foundation of China (Nos. 10775061, 11175054, 11675066, 11665019, and 11947229), the China Postdoctoral Science Foundation (No. 2019M663853), the Fundamental Research Funds for the Central Universities (Nos. lzujbky-2017-ot04 and lzujbky-2020-it01), and Feitian Scholar Project of Gansu Province.

✉ Hong-Fei Zhang
zhanghongfei@lzu.edu.cn

1 School of Nuclear Science and Technology, Lanzhou University, Lanzhou 730000, China

2 Joint Department for Nuclear Physics, Institute of Modern Physics, CAS and Lanzhou University, Lanzhou 730000, China

3 Engineering Research Center for Neutron Application, Ministry of Education, Lanzhou University, Lanzhou 730000, China

relativistic mean-field (RMF) calculations with $Z = 120$, $N = 172, 184, 228$ [19–21] and the Hartree-Fock-Bogoliubov (HFB) model, with $Z = 124, 126$, $N = 162$ et al. [22, 23]. In practice, many model calculations predict the existence of a closed spherical shell at $N = 184$. Nevertheless, there is no consensus among theorists regarding which nuclide should be the next double-magic nucleus after $^{208}_{82}$Pb. At present, one of the most reliable methods is to further improve the theoretical calculation accuracy by using constantly enriched and updated experimental data to provide more reliable predictions for the properties of SHN.

In recent years, an updated macroscopic-microscopic Weizsäcker-Skyrme mass formula [24] referred to as WS* was developed, in which the constraint between mirror nuclei was considered. The root mean square (rms) deviation with respect to the 2149 masses [25] is reduced to 441 keV, which is one of the best results to date. Another important advantage is the ability to provide reasonable mass extrapolations for exotic and heavy nuclei. Hence, it is necessary to use the calculations from the WS* to further explore [26] the features of SHN around the predicted "island of stability," starting with the properties of the isotopic chain at $Z = 114$.

The remainder of this paper is organized as follows. In Sect. 2, the theoretical framework of the mass model and relatively detailed formulas of microscopic potential are presented. The detailed calculations and discussion are presented in Sect. 3. Finally, Sect. 4 summarizes the findings of the study. All the macro- and micro-physical quantities provide a vital signal that $^{298}_{114}$Fl as a spherical double-magic nucleus is the center of the SHN.

2 Theoretical descriptions

In Ref. [24], Wang et al. proposed a semiempirical nuclear mass formula based on the macroscopic-microscopic method [27, 28], i.e., WS*. The total energy of a nucleus can be written as the sum of the liquid-drop energy and microscopic energy and the Strutinsky shell correction:

$$E(A, Z, \beta) = E_{\mathrm{LD}}(A, Z) \prod_{k \geq 2} \left(1 + b_k \beta_k^2\right) + E_{\mathrm{mic}}(A, Z, \beta). \tag{1}$$

Z and A are the nuclear charge number and mass number, respectively. The liquid-drop energy of a spherical nucleus E_{LD} is described by a modified Bethe-Weizsäcker mass formula, and more details can be found in Ref [24]. The term $\prod_{k \geq 2} \left(1 + b_k \beta_k^2\right)$ is the result of the Skyrme energy density functional together with the Thomas-Fermi approximation [15], where β_k denotes the deformation parameters.

To obtain the microscopic energy E_{mic} or the nuclear single-particle energy levels, we take the standard form of the potential with the central Woods-Saxon term, the spin-orbit term, and (in the case of protons) with the electrostatic Coulomb term. The Schrödinger equation was solved using an approximate method [29, 30]. The single-particle Hamiltonian can be written as:

$$H = T + V + V_{\mathrm{so}}. \tag{2}$$

The spin-orbit potential takes the form of

$$V_{\mathrm{so}} = \lambda \left(\frac{\hbar}{2Mc}\right)^2 \times \nabla V \cdot (\vec{\sigma} \times \vec{p}), \tag{3}$$

where λ denotes the strength of the spin-orbit potential and considers the isospin dependence in the form $\lambda = \lambda_0 \left(1 + \frac{N_i}{A}\right)$ with $N_i = Z$ for protons and $N_i = N$ for neutrons. The central Woods-Saxon potential takes the form:

$$V = \frac{V_q}{1 + \exp\left[\frac{r - \mathcal{R}(\theta)}{a}\right]}, \tag{4}$$

where the depth of the central potential ($q = p$ for protons and $q = n$ for neutrons) can be written as

$$V_q = V_0 \pm V_s I \tag{5}$$

with the plus sign for neutrons and the minus sign for protons. a is the surface diffuseness parameter of the single-particle potential. $\mathcal{R}(\theta)$ is equal to the distance from the origin of the coordinate system to a point on the nuclear surface.

$$\mathcal{R}(\theta) = c_0 R[1 + \beta_2 Y_{20}(\theta) + \beta_4 Y_{40}(\theta) + \beta_6 Y_{60}(\theta)] \tag{6}$$

with the scale factor c_0, which represents the incompressibility effect of nuclear matter in the nucleus and is determined by the so-called constant volume condition [29]. $R = r_0 A^{1/3}$ is the radius of the spherical nucleus of an identical volume (with the same value for protons and neutrons). $Y_{\mathrm{lm}}(\theta, \phi)$ are spherical harmonics. For protons, the Coulomb potential was also involved (see Ref. [29, 30] for details). It should be noted that to increase the credibility of extrapolations in the macroscopic-microscopic approach, the symmetry potential V_s in the WS* is the same as the macroscopic symmetry energy coefficient a_{sym}, which bridges the relationship between the macroscopic and microscopic parts.

The macroscopic term is only able to reproduce the smooth trend of binding energy, but not local fluctuations. Hence, in addition to the smooth trend, the microscopic energy is considered for the local fluctuations [31]. The most important of these fluctuations stems from shell effects. To extract the shell correction, a practical Strutinsky's prescription [32, 33] is applied in the calculation of $E_{\min}$, which takes the form of

$$E_{\mathrm{mic}} = c_1 E_{\mathrm{shell}} + |I| E'_{\mathrm{shell}}, \tag{7}$$

where E_{shell} is equal to the sum of the shell corrections for neutrons and protons. E'_{shell} denotes the shell correction energy of the mirror nucleus. The term $|I|E'_{\mathrm{shell}}$ takes into account the mirror nuclei constraint and isospin-symmetry-breaking effect [24]. c_1 denotes the scale factor.

3 Results and discussion

The one- and two-nucleon separation energies indicate how difficult it is to peel off one and two nucleons from the parent nucleus. Hence, one and two neutron (proton) separation energies can be extracted from the nuclear binding energies (B) by using the definition $S_{\mathrm{n;2n}}(N,Z) = B(N,Z) - B(N-n;2n,Z)$, $S_{\mathrm{p;2p}}(N,Z) = B(N,Z) - B(N,Z-p;2p)$. The most striking application is to obtain information about the shell structure. In particular, the separation energies of two nucleons are useful for finding new magic numbers in super-heavy and exotic nuclei [34, 35]. Owing to the powerful extrapolation ability of the macroscopic-microscopic nuclear mass formula, one can extrapolate nuclear masses for unknown nuclei based on theoretical mass models. Here, we calculated the binding energy of the nuclei around $Z = 114$ and $N = 184$ from the WS* to investigate the physical properties of the $Z = 114$ isotopic chain and $N = 184$ isotonic chain.

The one- and two-nucleon separation energies of the $Z = 114$ isotopic and $N = 184$ isotonic chains of the WS* [24] are shown in Fig. 1, labeled as (a) and (b), respectively, and used to find the magic numbers. The experimental data [36] and theoretical calculations using the finite-range droplet model (FRDM2012) [37] are also included for comparison, where red, black, and purple symbols denote the results of the WS*, FRDM2012, and experimental data, respectively. As shown in Fig. 1a, the agreement between the WS* and experimental data is good. There are only small differences between these two curves, but the trends are consistent. The values of S_{n} and $S_{2\mathrm{n}}$ show a decreasing trend with an increase in the neutron number. In addition, S_{n} shows an obvious even-odd stagger effect. Furthermore, the calculations of these two theories are consistent with each other. With careful observation, it can be found that both have a larger downward slope between $N = 184$ and $N = 185$, implying that for the $Z =$ 114 isotopic chain, the nucleus is more stable at a neutron number of 184. In addition, the results of the FRDM2012 in Fig. 1a have an unusual tendency to jitter violently at neutron numbers 197 and 199 because the deformation value β_2 changes violently from less than 0.1 at 196 to more than 0.54 at neutron numbers 197 and 198 and finally returns to normal after 199. A similar trend can be seen between $Z = 114$ and $Z = 115$ in Fig. 1b, and the trend of proton separation energy curve of the WS* is also very consistent with the FRDM2012, which are nearly in superposition with each other. For $N = 184$ isotonic chain, $Z = 114$ is the magic proton number and for $Z = 114$ isotopic chain $N = 184$ is the magic neutron number.

It is also interesting to explore the α-decay energies ($Q_\alpha = B(\alpha) + B(Z-2, A-4) - B(Z,A)$) to determine the magic numbers. Figure 2 contains the α-decay energies Q_α that are calculated with experimental [36], the WS* [24], and FRDM2012 [37] for $Z = 114$ isotopic and $N = 184$ isotonic chains, marked (a) and (b), respectively. It can be seen that the downward trend of WS* in Fig. 2a is essentially the same as the experimental trend, but the slopes between them are slightly different. Meanwhile, we find a dramatic turning point of the α-decay energy curve at $N =$ 184 for both theories, where the predicted neutron shell closure appears as a local minima in the curve. In addition, these results are very similar to other theoretical calculations, for example, in the second graph of Ref. [10], the trend of the theoretically predicted Q values for α decays between $171 < N < 175$ on the $Z = 114$ isotopic chain remains consistent with the experimental data, and this theoretically predicted Q value also maintains a continuing decreasing trend as the neutron number continues to increase toward $N = 184$. Such a significant decreasing trend is due to the effect of the closed neutron shell, despite the fact that the obtained heavy isotopes of Fl are still far from $N = 184$ by eight neutrons. In Fig. 2b, there is a tendency for the Q_α calculated by the two theories to increase as the number of proton increases, where the number of proton Z continues to increase rapidly from 114 to 116. As a result, the conclusion that $^{298}_{114}$Fl is a double-magic nucleus is verified again.

Based on the conclusions given above, it is necessary to calculate the rms deviations of the binding energies, one- and two-neutron (proton) separation energies, and α-decay energies of heavy and super-heavy nuclei corresponding to WS*. The experimental data needed for calculation here are those derived from the experimental binding energies [36] of $Z \geq 82$ and $N \geq 126$ (the standard deviation uncertainty of the mass is less than or equal to 150 keV). The corresponding results are listed in Table 1. We find that all rms deviations are very small, which further confirms the conclusion that $Z = 114$ is the magic proton number of the $N = 184$ isotonic chain and $N = 184$ is the magic neutron number of the $Z = 114$ isotopic chain.

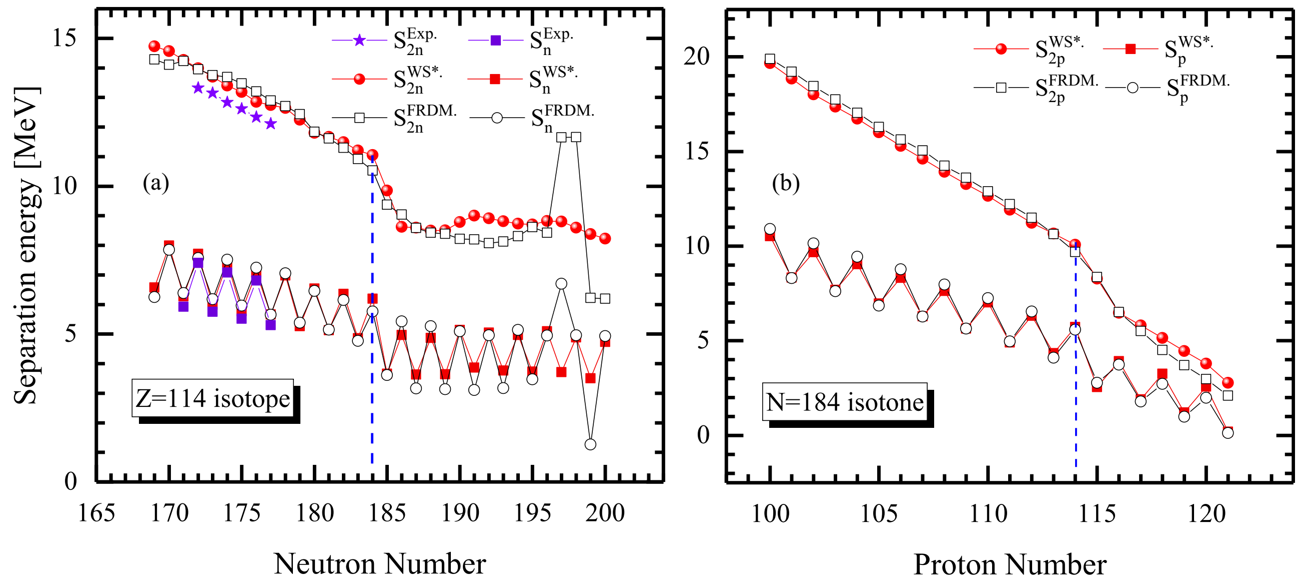

Fig. 1 (Color online) **a** The one- and two-neutron separation energies of $Z = 114$ isotopic chain obtained by the WS* [24], FRDM2012 [37], and experimental [36], labeled with solid red, open black and solid purple, respectively. The lower right corner label indicates whether it counts one- or two-nucleon separations and is accompanied by a different shape. **b** One- and two-proton separation energies of the $N = 184$ isotonic chain obtained by WS* [24] and FRDM2012 [37]. The marking rules are the same as those in **a**. (The unit of the ordinate is MeV)

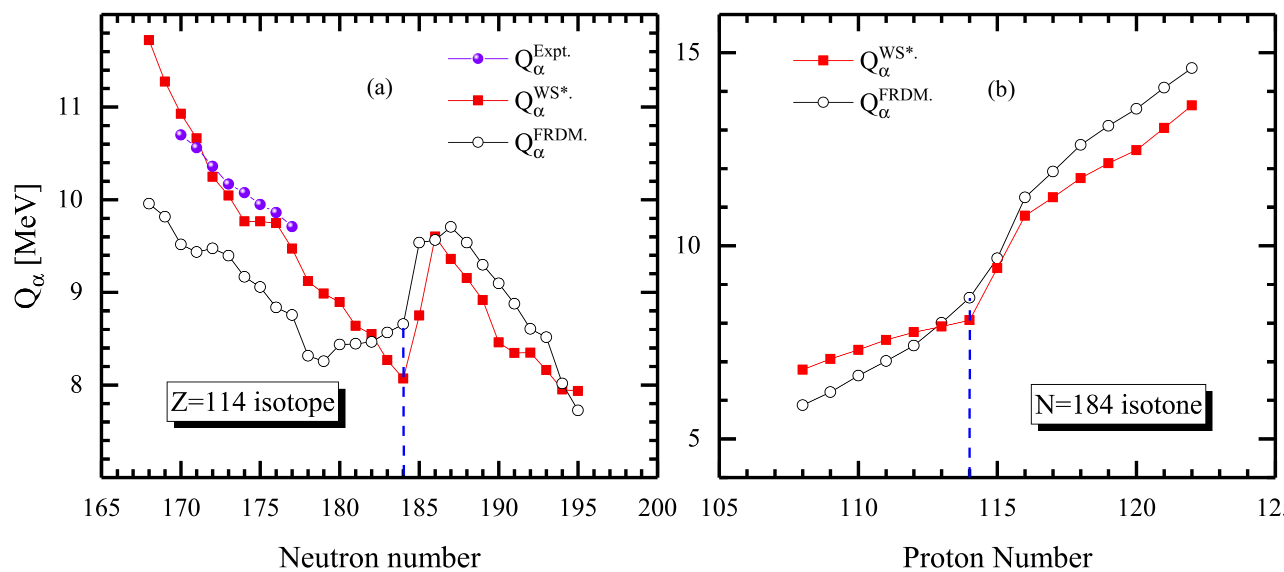

Fig. 2 (Color online) **a** The α-decay energies Q_α of $Z = 114$ isotopic chain obtained by the WS* [24], FRDM2012 [37], and experimental [36], labeled with solid red square, open black circle and solid purple circle, respectively. **b** The same as **a**, but for the $N = 184$ isotonic chain. (The unit of the ordinate is MeV)

Table 1 This table shows the rms deviations of the binding energies (E_b), one- and two-neutron (proton) separation energies (S_n, S_{2n}, S_p, S_{2p}), α-decay energies (Q_α) of heavy and super-heavy nuclei corresponding to the WS*

E_b	S_n	S_{2n}	S_p	S_{2p}	Q_α
490	177	222	209	295	294

From the macro-physical properties above, it can be concluded that $^{298}_{114}$Fl is a double-magic nucleus. Moreover, the properties of $^{298}_{114}$Fl from the microscopic energy-level structure are worth investigating. The spherical single-particle energy levels of protons and neutrons of $^{298}_{114}$Fl corresponding to the WS* parameters are calculated in a Woods-Saxon potential well with the spin-orbit term. The results are shown in Fig. 3, in which the left half belongs to

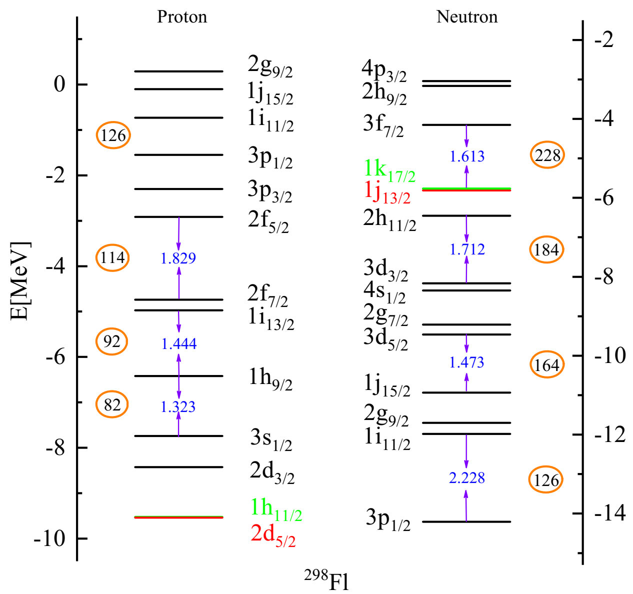

Fig. 3 (Color online) The single-particle levels of the nuclide ^{298}Fl. The left half shows the energy levels of the proton and the right for neutrons (in MeV)

protons and the right half belongs to neutrons. The number in the orange ellipse on both sides represents the number of nucleons that fill the energy level below it, which is the closest to it and has given the energy difference of the corresponding energy levels with blue numbers. The energy level signs with a color corresponding to the energy levels with the same color to facilitate the distinction. From this figure, we can see that the gap of $Z = 114$ with a difference of 1.829 MeV is the largest for the protons of $^{298}_{114}$Fl, and no significant gap between the levels at $Z = 126$ appears. Then, turning to the neutron shell structure, the gap $N = 184$ is one of the biggest gaps, corresponding to a difference of 1.712 MeV. The relation between the number of neutrons N or protons Z and the mass number A of a beta-stable nucleus is obtained according to the formula $N - Z = 0.4A^2/(A + 200)$ [38]. The nucleus $^{298}_{114}$Fl is also very close to the extrapolated beta-stability line. In addition, the equilibrium deformation β_2, β_4, and β_6 are obtained by searching for the minimum binding energy using the optimized DSC method. Theoretically, the ability to describe SHN properties is enhanced by using a three-dimensional deformation space. A contour map of the microscopic energy E_{mic} of the nucleus $^{298}_{114}$Fl calculated from WS* as a function of deformation β_2 and β_4 is shown in Fig. 4. At each point (β_2; β_4), the energy is minimized in β_6 degrees of freedom. As shown in the figure, for nucleus $^{298}_{114}$Fl, there is a local spherical minimum, with β_2 and β_4 being almost zero. The calculated β_2, β_4, and β_6 for the nucleus $^{298}_{114}$Fl in WS* are equal to –0.0002, 0.0001, and –0.0001, respectively. All these deformation values

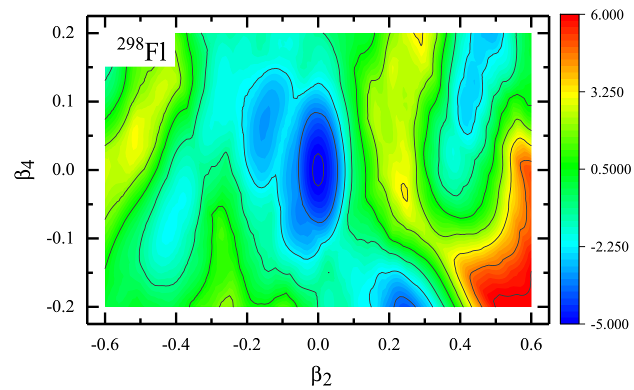

Fig. 4 (Color online) Contour map of the microscopic energy E_{mic} calculated from WS* for nucleus ^{298}Fl as a function of deformation β_2 and β_4. At each point (β_2; β_4), the energy is minimized in β_6 degrees of freedom (in MeV)

indicate that the ground state is spherical. From these calculations, it can be seen that $^{298}_{114}$Fl is a spherical double-magic nucleus.

To further demonstrate the accuracy of the theory, a graph of the sum of the shell corrections of protons and neutrons calculated using WS* to the nuclear macroscopic potential energies is shown in Fig. 5, where the deformation values of each nucleus are chosen for its corresponding lowest equilibrium deformation. The black circles in the figure represent the super-heavy nuclei with $Z > 104$ that have been synthesized experimentally to date. Three local minima can be observed in the figure, which is in the vicinity of the double-magic nuclei ^{208}Pb, ^{270}Hs, and ^{298}Fl, for the region above $N > 176$, the minima fall on the nucleus $^{298}_{114}$Fl; furthermore, it has been experimentally confirmed by decay energies that the nucleus ^{270}Hs is a double-magic deformed nucleus [39–41]. For the double-magic nucleus ^{270}Hs, as before, the single-particle energy levels obtained using WS* and a contour map of the

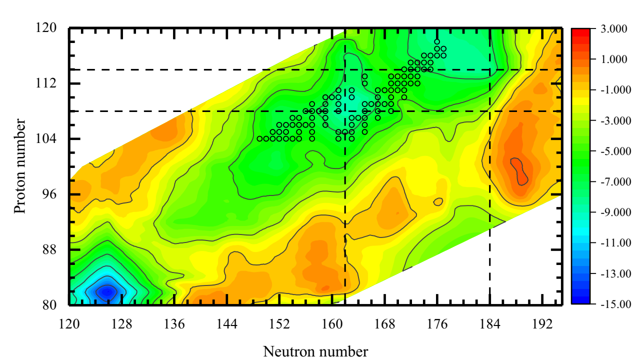

Fig. 5 (Color online) The graph of the sum of the shell corrections E_{shell} of protons and neutrons to the nuclear macroscopic potential energy calculated using WS* (in MeV). The black circles in the figure represent the super-heavy nuclei with $Z > 104$ that have been synthesized experimentally thus far

microscopic energy similar to Fig. 4 are given in Figs. 6 and 7. First, Fig. 6 shows that the ground state of nucleus ^{270}Hs is deformed and is not a sphere, and WS* calculations show that its lowest equilibrium deformation values are $\beta_2 = 0.2154$, $\beta_4 = -0.0553$, $\beta_6 = -0009$. Later, in Fig. 7, the corresponding single-particle energy levels of the nucleus ^{270}Hs are shown at these deformation values, and it can be seen that the energy gaps are relatively significant at proton and neutron numbers filled to 108 and 162, respectively. The theory also confirms that ^{270}Hs is a double-magic deformed nucleus. It is worth noting that when deformations are not considered, that is, the shape of the nucleus if all are treated as spherical, the strong shell correction that the nucleus ^{270}Hs would have had at this point disappears, as can be seen in Fig. 6. By using a multidimensional deformation space, the magic deformed nucleus ^{270}Hs is reproduced, and the region surrounding it connects the double-magic nucleus ^{208}Pb with the predicted SHN around $^{298}_{114}$Fl. As shown in Fig. 5, the new image within the region of super-heavy nuclei can be likened to two connected peaks on which these now-synthesized super-heavy nuclei are spread exactly.

In the absence of super-heavy nuclear data at the time, the possible magic numbers were found to be $Z = 114$ and $N = 184$ in Ref. [16]. This seems to be the first time that the Woods-Saxon potential has been used to describe the structure of a nucleus. Inspired by this article, we calculated the shell structure in a manner similar to Ref. [16] with the WS* parameters used for comparison. The calculation was performed for the mass numbers $A = 209$, 275, 299, and 355 with proton numbers $Z = 83$, 107, 115, and 127, respectively. The results are shown in Fig. 8, where the left half shows energy levels for protons and the right for neutrons. As shown in the left half of the figure, the energy gap at $Z = 82$ becomes narrower as the number

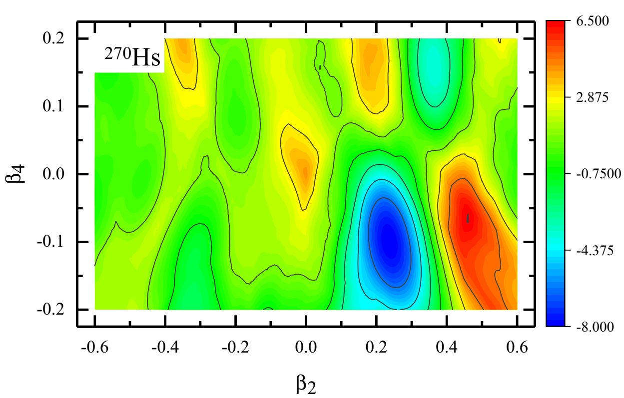

Fig. 6 (Color online) Contour map of the microscopic energy E_{mic} calculated using WS* for nucleus ^{270}Hs as a function of deformation β_2 and β_4. At each point (β_2; β_4), the energy is minimized in β_6 degrees of freedom (in MeV)

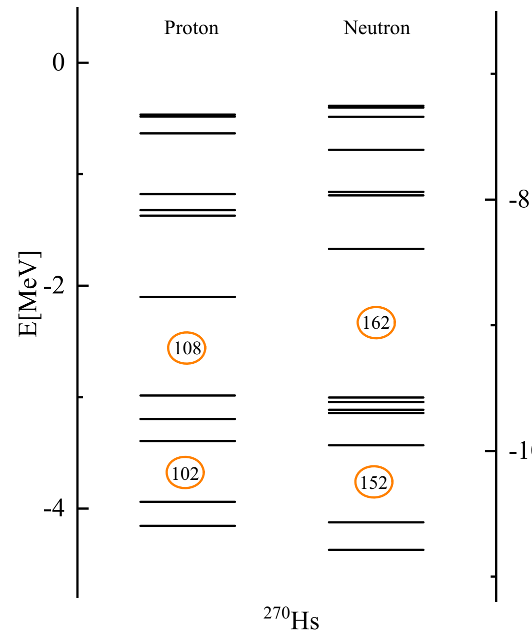

Fig. 7 (Color online) The single-particle levels of the nuclide ^{270}Hs. The left half shows the energy levels of the proton and the right half shows the energy levels for neutrons (in MeV)

of masses increases, but the gap is still relatively large over a large range. Starting from mass number 300, there is no significant gap between the levels at $Z = 126$, indicating that in the super-heavy nuclear region, the well-known magic number 126 is no longer effective for protons. Instead, a larger shell gap appears in the parameter set at $Z = 114$, which can be considered as a magic number. For the neutrons shown in the right half of the figure, the traditional $N = 126$ and $N = 184$ magic numbers still exist throughout the heavy and super-heavy nuclei region. In addition, for neutrons, it is found that the shell gap of $N = 228$ increases as the mass number increases, which can also be considered as a magic number. These findings are in good agreement with those reported in Ref. [16], where they both give consistent magic numbers. In other words, this study can be regarded as the verification and expansion of Ref. [16]. In particular, we reproduce all the results of WS* to ensure our correctness, such as the single-particle levels.

For heavy and super-heavy nuclei, α-decay is the main decay mode [42]. Moreover, it is also a probe for experimentally exploring the nature of SHN. Accordingly, we calculate the half-lives of the α-decay for the $Z = 114$ isotopic chain and the $N = 184$ isotonic chain. To compute the α-decay half-lives, the latest improved formula proposed by Deng et al. [43–45] was used, which is expressed as:

$$\log_{10} T_{1/2} = a + bA^{1/6}\sqrt{Z} + c\frac{Z}{\sqrt{Q_\alpha}} + dl(l+1) + h, \quad (8)$$

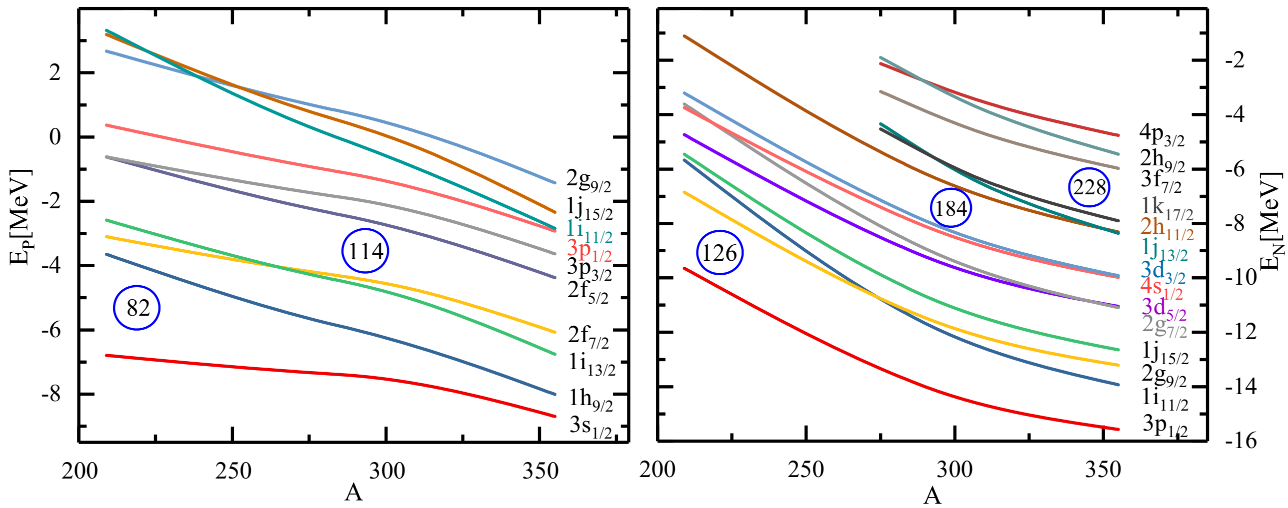

Fig. 8 (Color online) Energies levels of the proton (left) and neutron (right) versus mass number A. These calculations were performed for the mass numbers $A = 209, 275, 299,$ and 355 with proton numbers $Z = 83, 107, 115,$ and 127, respectively

where the first three terms are the same as those in the original Royer formulas. The fourth term represents the contribution of the centrifugal potential. l is the angular momentum removed by the α particle. The fifth term represents the blocking effect of unpaired nucleons. More details can be found in Ref. [45]. Moreover, a recent study calculated the uncertainties in the empirical formulae for the α decay half-lives of heavy and super-heavy nuclei[46]. The values of spin and parity of nuclei are obtained from calculations of odd-nucleon spin and parity at the nuclear ground state by P. Möller [47]. The results are shown in Fig. 9, where the red, black, purple symbols denote the calculations using the WS* [24], FRDM2012 [37], and experimental data [36], respectively. In addition, the blue symbols in Fig.9a denote the calculated half-lives with experimental Q_α to test the reliability of Eq. (8). It can be seen that the calculated α-decay half-lives from experimental Q_α coincide almost perfectly with the experimental half-lives, implying that, as long as we have the right Q_α, the presently used method can give precise results for α-decay half-lives. It can be observed from Fig. 9a that the predicted half-lives curves of α-decay obtained using the two theories basically have the same trend for $Z = 114$

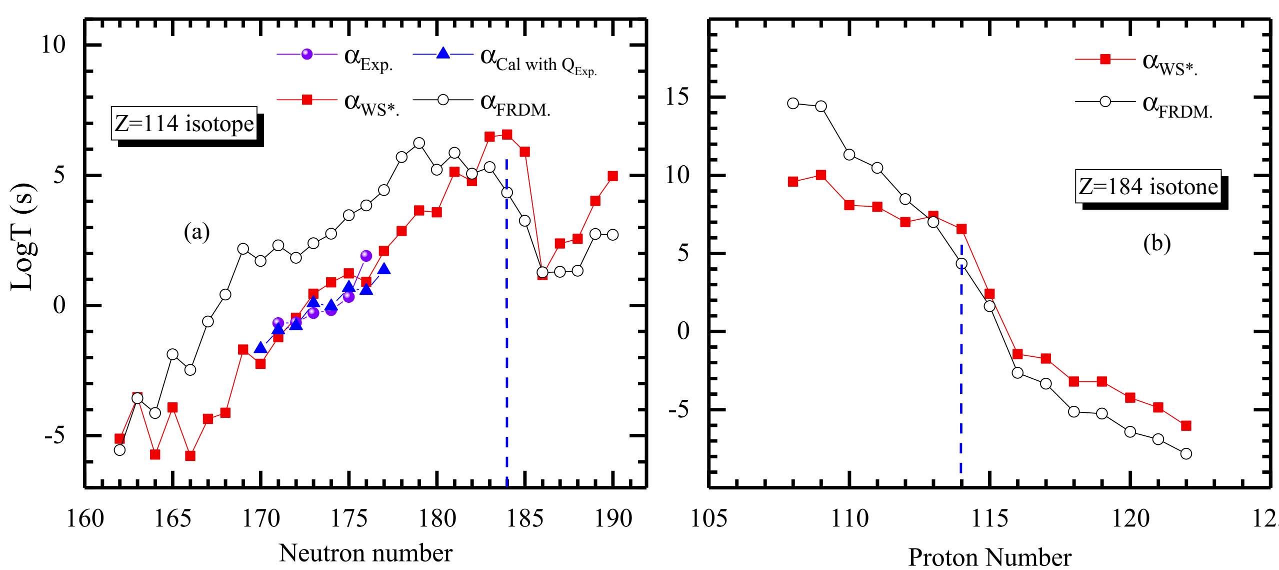

Fig. 9 (Color online) (a) The predicted logarithmic α-decay half-lives of $Z = 114$ isotopic chain using Eq. (8) with Q_α obtained by the WS* [24], FRDM2012 [37], and experimental [36], labeled with solid red squares, open black circles, and solid blue triangles, respectively. (b) The same as (a), but for the $N = 184$ isotonic chain. (The unit of the ordinate is second) The solid purple circle in figure (a) denotes the experimental α-decay half-lives

isotopic chain, but the results of FRDM2012 are generally higher for $N = 182$. The WS* results were generally in good agreement with the experimental data. In particular, when the neutron number N crosses $N = 184$ for WS*, the predicted α decay half-lives decrease sharply, and at $N = 186$, α decay half-lives are reduced by more than four orders of magnitude. This indicates that strong shell effects were reflected. Its half-life does not decrease much at $N = 185$ compared with $N = 184$ because of the blocking effect of unpaired neutrons and the fact that the angular momentum carried by the α particle during decay is as high as 5, which extends its half-life to some extent. The α-decay half-life of $^{298}_{114}$Fl is approximately 42.5 days with Q_α of WS* and approximately 6 h with Q_α of the FRDM2012. Fig. 9b plots the logarithms of calculated half-lives of the two theories for $N = 184$ isotonic chain. From this figure, we can see that when the proton number $Z > 114$ for WS*, the predicted α decay half-lives drop dramatically by eight orders of magnitude at $Z = 116$. As for FRDM2012, its theoretical predictions are very similar to the results given by WS* but have an overall trend opposite to that of Fig. 2b.

A systematic study of shell energy gaps calculated using a variety of theoretical models was recently launched in Ref. [48], where WS* similarly gives results for $Z = 114$ and $N = 184$ as the two obvious magic numbers. Moreover, experimental results show the existence of nuclear shell effects near $Z = 114$, as given in the fourth figure of Ref. [41], where the experimentally measured trend of the total evaporation-residue cross section of the hot fusion becomes locally maximum near $Z = 114$ supports this point. Similarly, the fourth figure in Ref. [49] shows that the maximum cross section measured for the experimentally synthesized lighter isotopes of Fl decreases sharply with smaller neutron numbers. The fifth figure in Ref. [49] shows the experimental and theoretical spontaneous fission half-lives of even-even nuclei in the super-heavy region, and it can be seen that both shells $N = 152$ and 162 have a strong influence on the spontaneous fission of the isotopes of No and Rf-Hs, whereas a similar stabilizing influence of the $N = 184$ shell also seems apparent for Cn and Fl. Recent experiments have also shown that the element Fl is a volatile metal[50]. In addition, because the combination of stable nuclei does not provide such neutron-rich nuclei for the synthesis of super-heavy nuclei with $N > 184$, it is hoped that in the future it will be possible to make use of secondary beams and, if possible, to synthesize $^{298}_{114}$Fl by obtaining compound nuclei with neutron numbers above 300 [51]. Some theoretical studies on super-heavy nuclei $Z = 110 \sim 125$ have also been reported [52–61].

4 Summary

In summary, the existence of an "island of stability" among the super-heavy elements is a fundamental prediction of modern nuclear theory, and this stability island has not yet been localized experimentally. Inspired by Ref. [16], we have approached the study of stability island in super-heavy elements starting from the properties of the $Z = 114$ isotopic chain. The experimental binding energies, one- and two-neutron (proton) separation energies, and α-decay energies were compared with the calculations obtained using the WS* for heavy and super-heavy nuclei, and the agreement was excellent. The features of one- and two-nucleon separation energies and α-decay energies of the WS* and FRDM2012 both indicate that $Z = 114$ is the magic proton number of the $N = 184$ isotonic chain and $N = 184$ is the magic neutron number of the $Z = 114$ isotopic chain. Concurrently, the spherical single-particle levels of nucleus $^{298}_{114}$Fl were given using a Woods-Saxon potential well with a spin-orbit term [29, 30] and combined with the equilibrium deformation values (β_2, β_4, β_6) of nucleus $^{298}_{114}$Fl calculated by the WS* are essentially equal to zero, it can be seen that $^{298}_{114}$Fl is a spherical double-magic nucleus. Then, we calculated the shell structure in a manner similar to Ref. [16] with the WS* parameters, where the results are in good agreement with the results of Ref. [16]. In the final part, the latest formula is applied to predict the α-decay half-lives of the $Z = 114$ isotopic and $N = 184$ isotonic chains. In general, these microscopic and macroscopic physical properties obtained by exploring the nature of isotopic chains provide a positive signal that $^{298}_{114}$Fl is a spherical double-magic nucleus and also the center of the SHN.

References

1. Y.T. Oganessian, V.K. Utyonkov, Y.V. Lobanov et al., Measurements of cross sections for the fusion-evaporation reactions ^{244}Pu(^{48}Ca,xn)$^{292-x}$114 and ^{245}Cm(^{48}Ca,xn)$^{293-x}$116. Phys. Rev. C **69**, 054607 (2004)
2. Y.T. Oganessian, V.K. Utyonkov, S.N. Dmitriev et al., Synthesis of elements 115 and 113 in the reaction ^{243}Am+^{48}Ca. Phys. Rev. C **72**, 034611 (2005). https://doi.org/10.1103/PhysRevC.72.034611
3. Y.T. Oganessian, V.K. Utyonkov, Y.V. Lobanov et al., Synthesis of the isotopes of elements 118 and 116 in the ^{249}Cf and ^{245}Cm +^{48} Ca fusion reactions. Phys. Rev. C **74**, 044602 (2006). https://doi.org/10.1103/PhysRevC.74.044602
4. Ch.E. Düllmann, M. Schädel, A. Yakushev et al., Production and decay of element 114: high cross sections and the new nucleus ^{277}Hs. Phys. Rev. Lett. **104**, 252701 (2010). https://doi.org/10.1103/PhysRevLett.104.252701
5. J.M. Gates, Ch.E. Düllmann, M. Schädel et al., First superheavy element experiments at the GSI recoil separator TASCA: the

production and decay of element 114 in the ^{244}Pu (^{48}Ca,3–4n) reaction. Phys. Rev. C **83**, 054618 (2011). https://doi.org/10.1103/PhysRevC.83.054618
6. S. Hofmann, G. Münzenberg, The discovery of the heaviest elements. Rev. Mod. Phys. **72**, 733 (2000). https://doi.org/10.1103/RevModPhys.72.733
7. J. Dvorak, W. Brüchle, M. Chelnokov, R. Dressler et al., Doubly magic nucleus $^{270}_{108}$Hs$_{162}$. Phys. Rev. Lett. **97**, 242501 (2006). https://doi.org/10.1103/PhysRevLett.97.242501
8. Y.T. Oganessian, F.S. Abdullin, P.D. Bailey et al., Synthesis of a new element with atomic number $Z = 117$. Phys.Rev. Lett. **104**, 142502 (2010). https://doi.org/10.1103/PhysRevLett.104.142502
9. M. Schädel, Chemistry of the superheavy elements. Philos. Trans. R. Soc. London, Ser. A **373**, 20140191 (2015). https://doi.org/10.1098/rsta.2014.0191
10. P.A. Ellison, K.E. Gregorich, J.S. Berryman et al., New Superheavy Element Isotopes: $^{242}\mathrm{Pu}(^{48}\mathrm{Ca}, 5n)^{285}114$. Phys. Rev. Lett. **105**, 182701 (2010). https://doi.org/10.1103/PhysRevLett.105.182701
11. Y.T. Oganessian, A.V. Yeremin, A.G. Popeko et al., Synthesis of nuclei of the superheavy element 114 in reactions induced by ^{48}Ca. Nature **400**, 242–245 (1999). https://doi.org/10.1038/22281
12. P. Möller, J.R. Nix, W.D. Myers et al., Nuclear ground-state masses and deformations. At. Data Nucl. Data Tables **59**, 185–381 (1995). https://doi.org/10.1006/adnd.1995.1002
13. Y. Aboussir, J.M. Pearson, A.K. Dutta et al., Nuclear mass formula via an approximation to the Hartree-Fock method. At. Data Nucl. Data Tables **61**, 127 (1995). https://doi.org/10.1016/S0092-640X(95)90014-4
14. S. Goriely, N. Chamel, J.M. Pearson, Hartree-Fock-Bogoliubov nuclear mass model with 0.50 MeV accuracy based on standard forms of Skyrme and pairing functionals. Phys. Rev. C **88**, 061302 (2013). https://doi.org/10.1103/PhysRevC.88.061302
15. N. Wang, M. Liu, X.Z. Wu, Modification of nuclear mass formula by considering isospin effects. Phys. Rev. C **81**, 044322 (2010). https://doi.org/10.1103/PhysRevC.81.044322
16. A. Sobiczewski, F.A. Gareev, B.N. Kalinkin, Closed shells for Z>82 and N> 126 in a diffuse potential well. Phys. Lett. **22**, 500 (1966). https://doi.org/10.1016/0031-9163(66)91243-1
17. W.D. Myers, W.J. Swiatecki, Nucl. Phys. **81**, 1 (1966)
18. S.G. Nilsson, C.F. Tsang, A. Sobiczewski et al., On the nuclear structure and stability of heavy and superheavy elements. Nucl. Phys. A **131**, 1 (1969). https://doi.org/10.1016/0375-9474(69)90809-4
19. Y.K. Gambhir, A. Bhagwat, M. Gupta, α-decay half-lives of the observed superheavy nuclei ($Z = 108 - 118$). Phys. Rev. C **71**, 037301 (2005). https://doi.org/10.1103/PhysRevC.71.037301
20. M. Bender, α-decay chains of $^{289}_{175}$114 and $^{293}_{175}$118 in the relativistic mean-field model. Phys. Rev. C **61**, 031302 (2000). https://doi.org/10.1103/PhysRevC.61.031302
21. S.K. Patra, C.L. Wu, C.R. Praharaj et al., A systematic study of superheavy nuclei for $Z = 114$ and beyond using the relativistic mean field approach. Nucl. Phys. A **651**, 117 (1999). https://doi.org/10.1016/S0375-9474(99)00129-3
22. S. Goriely, M. Samyn, J.M. Pearson et al., Hartree-Fock mass formulas and extrapolation to new mass data. Phys. Rev. C **66**, 024326 (2002). https://doi.org/10.1103/PhysRevC.66.024326
23. S. Typel, B.A. Brown, Skyrme Hartree-Fock calculations for the α-decay Q values of superheavy nuclei. Phys. Rev. C **67**, 034303 (2003). https://doi.org/10.1103/PhysRevC.67.034313
24. N. Wang, Z.Y. Liang, M. Liu et al., Mirror nuclei constraint in nuclear mass formula. Phys. Rev. C **82**, 044304 (2010). https://doi.org/10.1103/PhysRevC.82.044304
25. G. Audi, A.H. Wapstra, C. Thibault, The Ame2003 atomic mass evaluation: (II). Tables, graphs and references. Nucl. Phys. A **729**, 337 (2003). https://doi.org/10.1016/j.nuclphysa.2003.11.003
26. J. Bardeen, L.N. Cooper, J.R. Schrieffer, Theory of superconductivity. Phys. Rev. **108**, 1175 (1957). https://doi.org/10.1103/PhysRev.108.1175
27. H.F. Zhang, L.H. Wang, J.P. Yin et al., Performance of the Levenberg-Marquardt neural network approach in nuclear mass prediction. J. Phys. G Nucl. Part. Phys. **44**, 045110 (2017). https://doi.org/10.1088/1361-6471/aa5d78
28. N.N. Ma, H.F. Zhang, X.J. Bao et al., Weizsäcker-Skyrme-type mass formula by considering radial basis function correction. J. Phys. G Nucl. Part. Phys. **42**, 095107 (2015). https://doi.org/10.1088/0954-3899/42/9/095107
29. S. Cwiok, J. Dudek, W. Nazarewicz et al., Single-particle energies, wave functions, quadrupole moments and g-factors in an axially deformed woods-saxon potential with applications to the two-centre-type nuclear problems. Comput. Phys. Commun. **46**, 379 (1987). https://doi.org/10.1016/0010-4655(87)90093-2
30. J. Damgaard, H.C. Pauli, V.V. Pashkevich et al., A method for solving the independent-particle Schrödinger equation with a deformed average field. Nucl. Phys. A **135**, 432 (1969). https://doi.org/10.1016/0375-9474(69)90174-2
31. P. Salamon, A.T. Kruppa, Curvature correction in Strutinsky's method. J. Phys. G Nucl. Part. Phys. **37**, 105106 (2010). https://doi.org/10.1088/0954-3899/37/10/105106
32. V.M. Strutinsky, F.A. Ivanjuk, A new definition of shell corrections to the liquid drop energy. Nucl. Phys. A **255**, 405 (1975). https://doi.org/10.1016/0375-9474(75)90688-0
33. M. Brack, H.C. Pauli, On Strutinsky's averaging method. Nucl. Phys. A **207**, 401 (1973). https://doi.org/10.1016/0375-9474(73)90355-2
34. J.J. Li, W.H. Long, J. Margueron et al., Superheavy magic structures in the relativistic Hartree-Fock-Bogoliubov approach. Phys. Lett. B **732**, 169 (2014). https://doi.org/10.1016/j.physletb.2014.03.031
35. J.J. Li, J. Margueron, W.H. Long et al., Magicity of neutron-rich nuclei within relativistic self-consistent approaches. Phys. Lett. B **753**, 97 (2016). https://doi.org/10.1016/j.physletb.2015.12.004
36. M. Wang, W.J. Huang, F.G. Kondev et al., The AME 2020 atomic mass evaluation (II). Tables, graphs and references. Chin. Phys. C **45**, 030003 (2021). https://doi.org/10.1088/1674-1137/abddaf
37. P. Möller, A.J. Sierk, T. Ichikawa et al., Nuclear ground-state masses and deformations: FRDM(2012). At. Data Nucl. Data Tables **109–110**, 1 (2016). https://doi.org/10.1016/j.adt.2015.10.002
38. A.E.S. Green, *Nuclear Physics* (McGraw-Hill Book Company, Inc, New York, 1955), p. 250
39. Y.A. Lazarev, Y.V. Lobanov, Y.T. Oganessian et al., Discovery of enhanced nuclear stability near the deformed shells $N = 162$ and $Z = 108$. Phys. Rev. Lett. **73**, 624 (1994). https://doi.org/10.1103/PhysRevLett.73.624
40. J. Dvorak, W. Brüchle, M. Chelnokov et al., Doubly magic nucleus $^{270}_{108}$Hs$_{162}$. Phys. Rev. Lett. **97**, 242501 (2006). https://doi.org/10.1103/PhysRevLett.97.242501
41. Y.T. Oganessian, V.K. Utyonkov, F.S. Abdullin et al., Synthesis and study of decay properties of the doubly magic nucleus ^{270}Hs in the ^{226}Ra + ^{48}Ca reaction. Phys. Rev. C **87**, 034605 (2013). https://doi.org/10.1103/PhysRevC.87.034605
42. H.F. Zhang, G. Royer, α particle preformation in heavy nuclei and penetration probability. Phys. Rev. C **77**, 054318 (2008). https://doi.org/10.1103/PhysRevC.77.054318

43. G. Royer, Alpha emission and spontaneous fission through quasi-molecular shapes. J. Phys. G Nucl. Part. Phys. **26**, 1149 (2000). https://doi.org/10.1088/0954-3899/26/8/305
44. G. Royer, Analytic expressions for alpha-decay half-lives and potential barriers. Nucl. Phys. A **848**, 279 (2010). https://doi.org/10.1016/j.nuclphysa.2010.09.009
45. J.G. Deng, H.F. Zhang, G. Royer, Improved empirical formula for α-decay half-lives. Phys. Rev. C **101**, 034307 (2020). https://doi.org/10.1103/PhysRevC.101.034307
46. H.C. Manjunatha, L. Seenappa, K.N. Sridhar, Uncertainties in the empirical formulae for alpha decay half-lives of heavy and superheavy nuclei. Eur. Phys. J. Plus **134**, 477 (2019). https://doi.org/10.1140/epjp/i2019-12838-0
47. Look Up Calculated Odd-Nucleon Spins and Parities at the Nuclear Ground State. https://t2.lanl.gov/nis/data/astro/molnix96/spidat.html
48. Q.H. Mo, M. Liu, N. Wang, Systematic study of shell gaps in nuclei. Phys. Rev. C **90**, 024320 (2014). https://doi.org/10.1103/PhysRevC.90.024320
49. V.K. Utyonkov, N.T. Brewer, Y.T. Oganessian et al., Experiments on the synthesis of superheavy nuclei ^{284}Fl and ^{285}Fl in the ^{239,240}Pu $+^{48}$ Ca reactions. Phys. Rev. C **92**, 034609 (2015). https://doi.org/10.1103/PhysRevC.92.034609
50. A. Yakushev, J.M. Gates, A. Turler et al., Superheavy element flerovium (Element 114) is a volatile metal. Inorg. Chem. **53**, 1624 (2014). https://doi.org/10.1021/ic4026766
51. Y. Aritomo, Possibility of synthesizing a doubly magic superheavy nucleus. Phys. Rev. C **75**, 024602 (2007). https://doi.org/10.1103/PhysRevC.75.024602
52. H.C. Manjunatha, K.N. Sridhar, N. Sowmya, Investigations of the synthesis of the superheavy element $Z = 122$. Phys. Rev. C **98**, 024308 (2018). https://doi.org/10.1103/PhysRevC.98.024308
53. H.C. Manjunatha, N. Sowmya, Decay modes of superheavy nuclei $Z = 124$. Int. J. Mod Phys E **27**, 1850041 (2018). https://doi.org/10.1142/S0218301318500416
54. N. Sowmya, H.C. Manjunatha, Competition between different decay modes of superheavy element $Z = 116$ and synthesis of possible isotopes. Braz. J. Phys. **49**, 874–886 (2019). https://doi.org/10.1007/s13538-019-00710-4
55. N. Sowmya, H.C. Manjunatha, Investigations on different decay modes of darmstadtium. Phys. Part. Nucl. Lett. **17**, 370–378 (2020). https://doi.org/10.1134/S1547477120030140
56. H.C. Manjunatha, K.N. Sridhar, A detail investigation on the synthesis of superheavy element $Z = 119$. Phys. Part. Nucl. Lett. **16**, 647–655 (2019). https://doi.org/10.1134/S1547477119060487
57. K.N. Sridhar, H.C. Manjunatha, H.B. Ramalingam, Search for possible fusion reactions to synthesize the superheavy element $Z = 121$. Phys. Rev. C **98**, 064605 (2018). https://doi.org/10.1103/PhysRevC.98.064605
58. N. Sowmya, H.C. Manjunatha, P.S. Damodara Gupta et al., Competition between cluster and alpha decay in odd Z superheavy nuclei $111 \leq Z \leq 125$. Braz. J. Phys. **51**, 99–135 (2021). https://doi.org/10.1007/s13538-020-00801-7
59. H.C. Manjunatha, Comparison of alpha decay with fission for isotopes of superheavy nuclei $Z = 124$. Int. J. Mod Phys E **25**, 1650074 (2016). https://doi.org/10.1142/S0218301316500749
60. N. Sowmya, H.C. Manjunatha, N. Dhananjaya et al., Competition between binary fission, ternary fission, cluster radioactivity and alpha decay of ^{281}Ds. J. Radioanal. Nucl. Chem. **323**, 1347 (2020). https://doi.org/10.1007/s10967-019-06706-3
61. H.C. Manjunatha, Theoretical prediction of probable isotopes of superheavy nuclei of $Z = 122$. Int. J. Mod. Phys. E **25**, 1650100 (2016). https://doi.org/10.1142/S0218301316501007